Hutnické listy – *Metallurgical Journal*
Speciální vydání / Special Issue, roč. / vol. LXXIX
ISSN Online: 3029-8350

Flow Under Control: Modelling of Electromagnetic Effects in Continuous Casting

Řízené proudění: Modelování elektromagnetických účinků při kontinuálním odlévání oceli

Yahea Ayoub[1], Pavel E. Ramirez Lopez[1,2], Sailesh Kesavan[1], Magnus Gustafsson[3], Christer Nilsson[4]

[1] Process Metallurgy Department, SWERIM AB, Aronstorpsvagen 1, SE 97 437, Luleå, Sweden. *Contact e-mail: yahea.ayoub@swerim.se
[2] KTH, Royal Institute of Technology, Brinellvägen 23, SE-100 44 Stockholm, Sweden; pavel.ramirez.lopez@swerim.se; pe2@kth.se
[3] Luleå university of technology, Laboratorievägen 14, SE-971 87, Luleå, Sweden; magnus.gustafsson@ltu.se
[4] SSAB EMEA AB, Svartöbrinken 20, SE-974 37, Luleå, Sweden; christer.nilsson@ssab.com

Abstract

This work presents a numerical study on the influence of localized electromagnetic braking (EMBr) in thin-slab continuous casting. A coupled model of molten steel flow and electromagnetic fields was developed using ANSYS Fluent with its magnetohydrodynamics (MHD) module. Magnetic field distributions were generated through a MATLAB user-defined function and mapped onto the casting mould. A Box-Behnken experimental design was used to systematically vary five parameters: field intensity, diameter, x- and z-placement, and casting speed, resulting in 41 simulations. Key flow characteristics were monitored, including meniscus velocity, jet behavior, and wall forces. Results show that near-inlet EMBr placement leads to reduced jet velocity, downward deflection, and damping of flow variables. In contrast, fields placed below the jet increase upward flow momentum, meniscus velocity, and steel level. Larger coil diameters and higher magnetic field intensities generally reduce all flow parameters and promote upward jet deflection. Regression models reveal strong nonlinear and interaction effects, particularly between vertical placement, intensity, and diameter. The study demonstrates that EMBr positioning and configuration have significant but complex effects on flow behavior in continuous casting, providing valuable insights for process control and quality improvement in steel production.

***Keywords**: continuous casting, electromagnetic braking, slab casting, computational model*

Abstrakt

Tato práce představuje numerickou studii vlivu lokálního elektromagnetického brzdění (EMBr) při kontinuálním odlévání tenkých pásů. Pomocí programu ANSYS Fluent a jeho modulu magnetohydrodynamiky (MHD) byl vyvinut propojený model proudění roztavené oceli a elektromagnetických polí. Rozložení magnetického pole bylo generováno prostřednictvím uživatelsky definované funkce v MATLABu a promítnuto na odlévací formu. Pro systematickou změnu pěti parametrů – intenzity pole, průměru cívky, polohy v osách x a z a rychlosti odlévání – byl použit experimentální design Box-Behnken, což vedlo k realizaci 41 simulací. Sledovány byly klíčové charakteristiky proudění, včetně rychlosti menisku, chování proudu a sil působících na stěny formy. Výsledky ukazují, že umístění EMBr v blízkosti vstupu snižuje rychlost proudu, způsobuje jeho odklon směrem dolů a tlumí jeho proměnné. Naopak pole umístěná pod proudem zvyšují hybnost proudu směrem nahoru, rychlost menisku a hladinu oceli. Větší průměry cívek a vyšší intenzity magnetické pole obecně snižují všechny parametry proudění a podporují odklon proudu směrem nahoru. Regresní modely odhalují silné nelineární a interakční účinky, zejména mezi vertikálním umístěním, intenzitou a průměrem cívky. Studie ukazuje, že umístění a konfigurace EMBr mají významné a komplexní dopady na chování proudění při plynulém odlévání, což poskytuje cenné poznatky pro řízení procesu a zlepšení kvality výroby oceli.

***Klíčová slova:** plynulé lití, elektromagnetická brzda, odlévání bram, výpočetní model*

Hutnické listy – *Metallurgical Journal*
Speciální vydání / Special Issue, roč. / vol. LXXIX
ISSN Online: 3029-8350

1. Introduction

Steel is primarily produced via two methods: the blast furnace route and the electric arc furnace process. Regardless of the chosen production route, both methods typically culminate in a shared final step, continuous casting. In this stage, molten steel is continuously poured into a water-cooled mould where it solidifies into semi-finished forms, such as slabs. [3] Since the invention of continuous casting in the 19th century, a variety of control techniques have been developed, aimed at optimizing process parameters to prevent severe defects like breakouts.

One such control strategy is local electromagnetic braking (EMBr), which aims to stabilize the flow field within the mould, thereby indirectly enhancing thermal uniformity and solidification quality. As described by [5], the local EMBr system typically features circular electromagnetic coils arranged perpendicular to the mould surface. When connected to a direct current (DC) source, these coils generate a static magnetic field that penetrates the molten steel within the mould as shown in **Fig. 1**. The primary function of the local EMBr is to reduce the velocity of the impinging jet from the submerged entry nozzle (SEN), promoting a more stable and controlled flow within the mould.

The paper pursues two main objectives:

- To develop a numerical model capable of coupling molten steel flow with electromagnetic fields within a thin-slab continuous casting mould.
- To utilize this model in conducting a systematic parametric study aimed at characterizing the influence of local electromagnetic braking on mould flow behaviour.

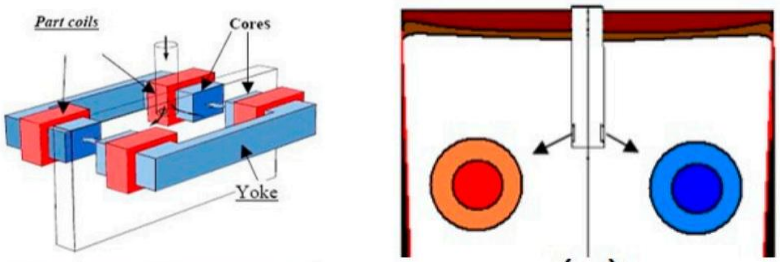

Fig. 1 An illustration of Local EMBr, according to [5]

Obr. 1 Ilustrace lokálního EMBr dle [5]

2. Method

To meet the objectives of this study, a numerical model of a thin-slab continuous casting mould was developed using ANSYS software. The geometry, depicted in **Fig. 2(a)**, was created in *ANSYS SpaceClaim* based on typical industrial dimensions for thin-slab caster. To enable a large number of simulations runs, the model was intentionally simplified to reduce computational cost.

The computational mesh, shown in **Fig. 2(b)**, was generated using *ANSYS Meshing*, while the flow and thermal simulations were configured in *ANSYS Fluent*. The model was further coupled with electromagnetic fields using Fluent's Magnetohydrodynamics (MHD) module, specifically through the induction equation method for simulating field-flow interaction.

Hutnické listy – *Metallurgical Journal*
Speciální vydání / Special Issue, roč. / vol. LXXIX
ISSN Online: 3029-8350

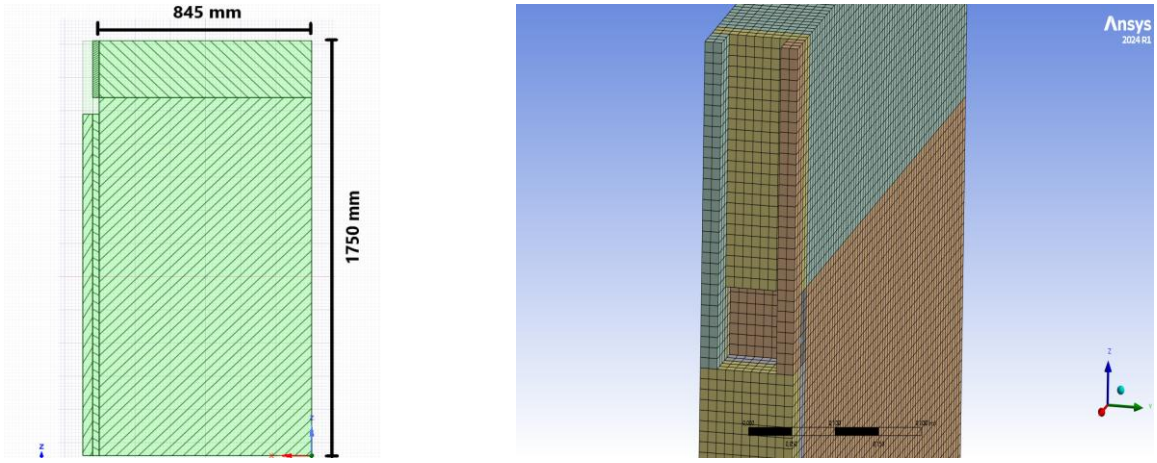

(a) (b)

Fig. 2 Model geometry and mesh-grid. A longitudinal cross section at y = 0.055 m [left]. A 3D view of the mesh-grid [right]

Obr. 2 Geometrie modelu a síť. Podélný řez v bodě y = 0,055 m [vlevo]. 3D pohled na síť [vpravo]

Three reference flow cases were simulated with three different casting speeds: 2,4 and 6 m/min, as illustrated in **Fig. 3**. The resulting jet trajectories were extracted and imported into *MATLAB*, as shown in **Fig. 4**, to guide the accurate placement of the magnetic field relative to the jet path. The magnetic field distributions were generated in *MATLAB* using a user-defined function (UDF) that allowed control over the field's intensity, shape, and location. The resulting data was exported as a .mag file, compatible with *ANSYS Fluent*, following the procedure outlined in the *ANSYS MHD Manual* [2].

A range of magnetic field configurations were applied to the fully developed flow fields, and the resulting jet behavior was monitored to systematically assess the influence of electromagnetic braking. The simulations were conducted using a transient model with a time step of 0.1 seconds. To account for the complex flow characteristics within the mould, turbulence was modeled using the standard k–ε model with standard wall functions, while multiphase flow was captured using the Volume of Fluid (VOF) method. The model included two phases, air and molten steel, with a surface tension coefficient of 1.2 N/m.

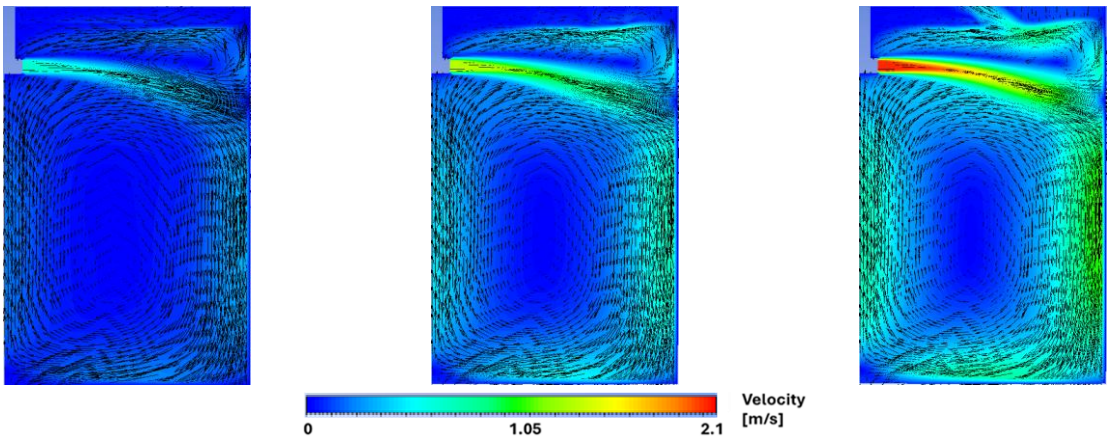

Fig. 3 Reference flow cases of three different casting speeds. 2 [m/min] [left], 4 [m/min] [middle] and 6 [m/min] [right]

Obr. 3 Referenční případy průtoku pro tři různé rychlosti lití: 2 [m/min] [vlevo], 4 [m/min] [uprostřed] a 6 [m/min] [vpravo]

Hutnické listy – *Metallurgical Journal*
Speciální vydání / Special Issue, roč. / vol. LXXIX
ISSN Online: 3029-8350

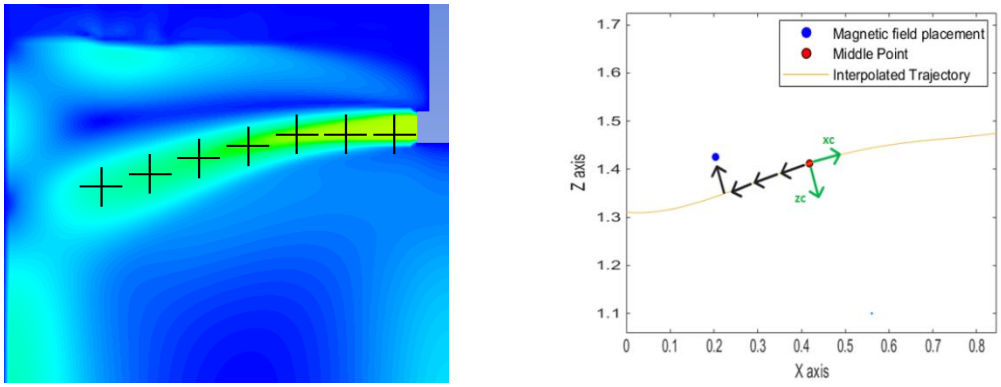

Fig. 4 Jet trajectory interpolation. The jet in Ansys Fluent [Left]. The jet interpolation in MATLAB [Right]

Obr. 4 Interpolace dráhy proudu. Proud v programu Ansys Fluent [vlevo]. Interpolace proudu v programu MATLAB [vpravo]

To systematically investigate the influence of key parameters on flow behavior, a Box-Behnken factorial design of experiments (DOE) was employed. Five independent variables were considered: magnetic field intensity, field diameter, horizontal (x) placement, vertical (z) placement, and casting speed. This resulted in a total of 41 simulation cases, spanning the parameter ranges summarized in **Tab. 1**.

Tab. 1 Overview of Field Intensity, Diameter, Distribution, Placement, and Casting Speed Ranges. U_{max} is the jet maximum velocity across a vertical line, this line is shown in red in Fig. 5

Tab. 1 Přehled rozsahů intenzity pole, průměru, rozložení, umístění a rychlosti lití. U_{max} je maximální rychlost proudu v průřezu svislou přímkou; tato přímka je na obr. 5 vyznačena červeně

DOE setup				
Xc placement [m]	**Zc placement [m]**	**Diameter [m]**	**Peak intensity [tesla]**	**Casting speed [m/s]**
-0.2	Where $\|u\| = -U_{max}/2$	0.1	0.1	2
0	0	0.3	0.3	4
+0.2	Where $\|u\| = +U_{max}/2$	0.5	0.5	6

Due to the absence of experimental measurement data for the local magnetic field distribution, the magnetic field was approximated using a two-dimensional Gaussian function. This analytical function was chosen for its smooth, symmetric profile, which is well-suited for representing localized magnetic fields. To match the desired field diameter and peak intensity, the Gaussian function was appropriately stretched and scaled. The general form of the function, along with the scaling operations applied, is presented in the following set of equations:

$$\sigma = \left(\frac{Diameter/2}{3}\right), \tag{1}$$

$$B_y(x,y,z) = \frac{A}{2\pi\sigma^2} e^{\left\{-\frac{(x-xcenter)^2+(z-zcenter)^2}{2\sigma^2}\right\}}, \tag{2}$$

With A such that:

$$B_y(x_{center}, y, z_{center}) = peak\_magnitude, \tag{3}$$

Hutnické listy – *Metallurgical Journal*
Speciální vydání / Special Issue, roč. / vol. LXXIX
ISSN Online: 3029-8350

Where x_{center} and z_{center} define the spatial location of the local EMBr field center, and $B_y(x_{center}, y, z_{center})$ represents the magnetic field component with maximum intensity.

Several key flow variables were monitored throughout the simulation runs to evaluate the effects of different magnetic field configurations. These variables are summarized below:

- Total force exerted on the narrow face of the mould
- Maximum velocity of the lower recirculation vortex
- Maximum molten steel meniscus level
- Maximum velocity magnitude at the meniscus
- Average velocity magnitude at the meniscus
- Average turbulent kinetic energy in the domain
- Maximum jet velocity along a specified line

Fig. 5 provides a detailed view of the locations where these variables were recorded. The molten steel level, along with both the maximum and average velocities at the meniscus, were evaluated across the *blue surface*, which corresponds to the region where the steel volume fraction equals 0.5, indicating the interface between air and steel. The total force on the narrow face was measured along the *green vertical surface*, representing the mould wall. Finally, the jet velocity and its deflection were recorded at the *yellow marker*, which also corresponds to the location of the maximum velocity magnitude along the *red reference line*.

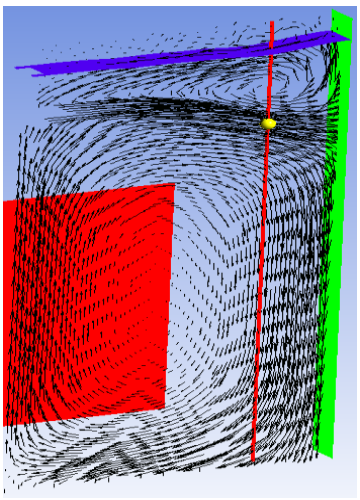

Fig. 5 Locations for measuring variables / **Obr. 5** Místa měření proměnných

3. Result

Fig. 6 displays the values of the monitored variables during two key time windows: 15 seconds before (plotted in green, blue and red for the casting speeds 2,4 and 6 m/min respectively) and 15 seconds after (plotted in black) the application of the magnetic fields at *t = 65 s*. A general trend observed immediately after EMBr activation is a sharp decrease in all monitored variables. However, this transient response is followed by a stabilization phase, with most variables reaching a new steady state around *t = 75 s*.

Hutnické listy – *Metallurgical Journal*
Speciální vydání / Special Issue, roč. / vol. LXXIX
ISSN Online: 3029-8350

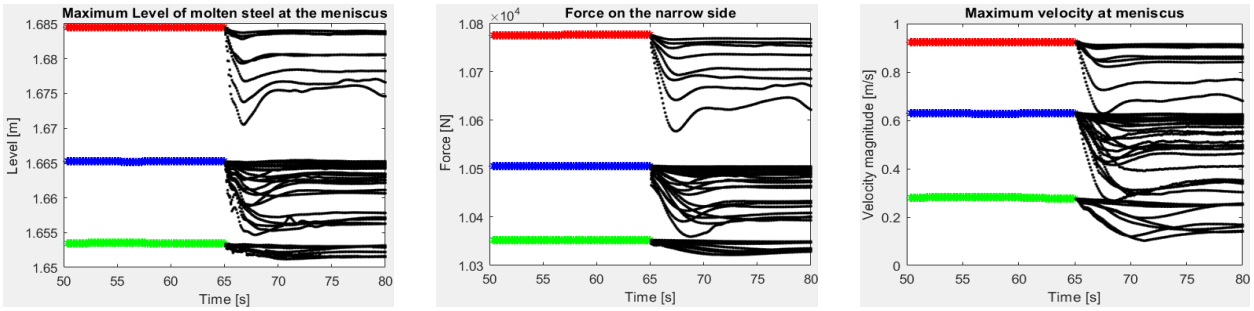

(a) (b) (c)

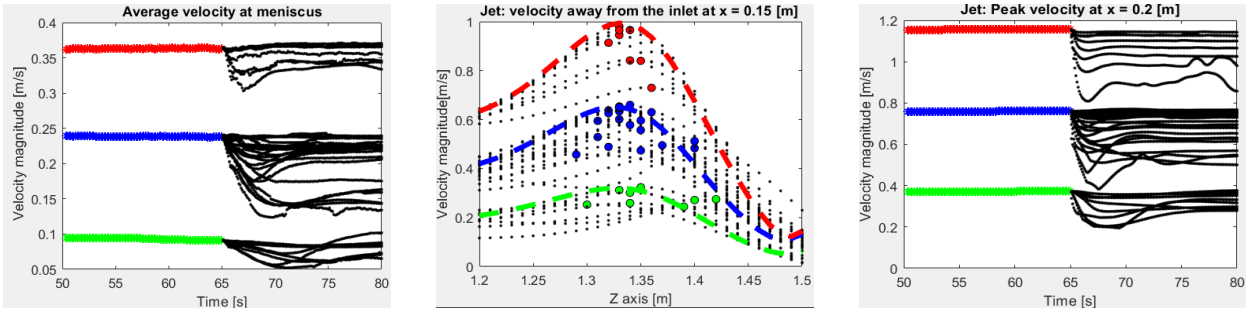

(a) (b) (c)

Fig. 6 Time variation of monitored variables: Green, blue, and red show casting speeds of 2, 4, and 6 m/min before the field is applied; black shows data during 41 magnetic field applications

Obr. 6 Časový průběh sledovaných veličin: zelená, modrá a červená barva znázorňují rychlosti lití 2, 4 a 6 m/min před zapnutím magnetického pole; černá barva znázorňuje data během 41 aplikací magnetického pole

Fig. 7 illustrates the maximum and minimum values achievable through the application of a local magnetic field, as predicted by the regression model fitted to the data shown in **Fig. 6**.

The results indicate that all monitored variables can be either increased or decreased relative to their reference values. The jet deflection ranges approximately ±0.10 m upward and 0.04 m downward. Additionally, the jet velocity can be reduced by approximately 75%, 45%, and 30% for casting speeds of 2, 4, and 6 m/min, respectively.

The molten steel level (standing wave height) decreases by more than 0.02 m at a casting speed of 6 m/min, while the force on the narrow side of the mould is reduced by about 100 N and 200 N at casting speeds of 2 and 6 m/min, respectively. Finally, the velocity of the upper recirculation vortex at the meniscus can be reversed at 2 m/min casting speed and reduced by approximately 50% at 6 m/min.

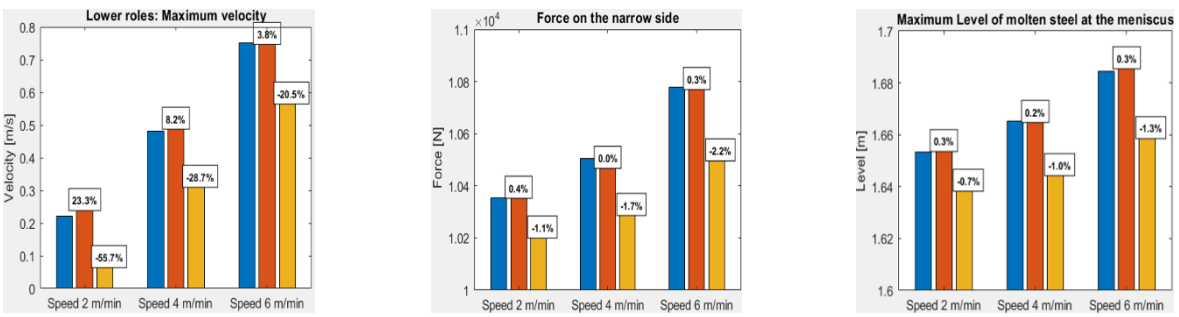

(a) (b) (c)

Hutnické listy – *Metallurgical Journal*
Speciální vydání / Special Issue, roč. / vol. LXXIX
ISSN Online: 3029-8350

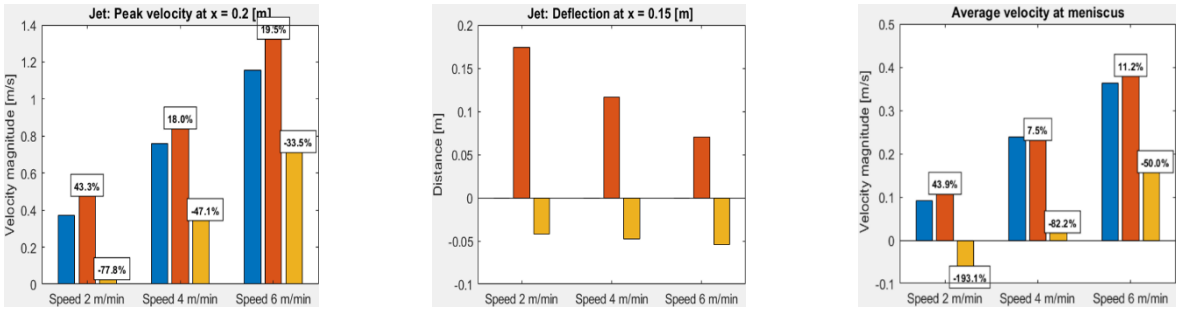

(d) (e) (f)

Fig. 7 This **Fig.** shows the maximum (red) and minimum (yellow) values of the regression model along with the percentage increase/decrease of the monitored variables reference value (blue)

Obr. 7 Tento obrázek znázorňuje maximální (červená) a minimální (žlutá) hodnoty regresního modelu spolu s procentuálním nárůstem/poklesem referenční hodnoty sledovaných veličin (modrá)

Fig. 8 presents a visual comparison between the reference flow field at a casting speed of 4 m/min and the flow field subjected to a local magnetic field. The application of local EMBr results in a substantial reduction in flow velocity within the upper recirculation vortex, accompanied by a noticeable decrease in the lower vortex velocity. Additionally, in panel (b), where a lower-intensity magnetic field is positioned closer to the submerged entry nozzle compared to panel (c), the jet demonstrates increased spreading, reduced deflection, and a more pronounced velocity reduction.

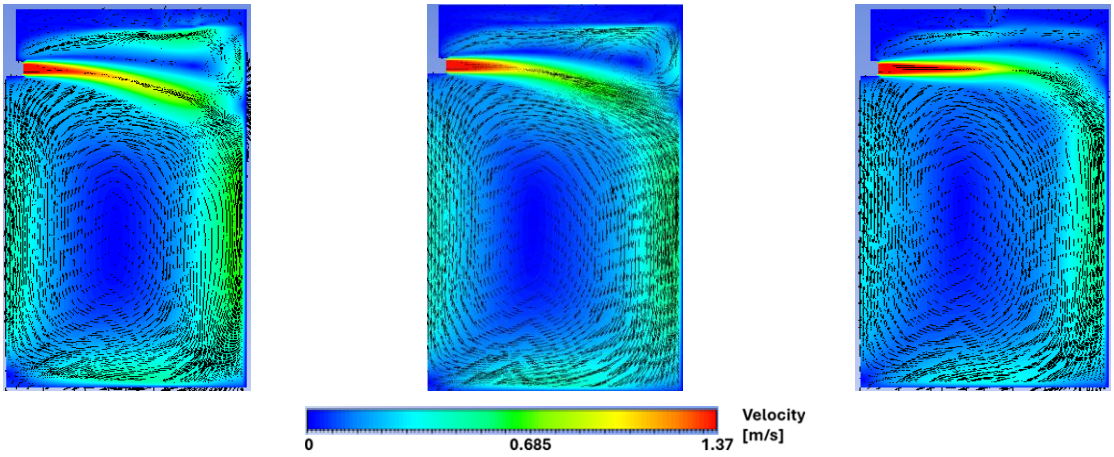

Fig. 8 [Left] Reference casting speed 4 [m/min]. [middle] The field was placed near the inlet and jet center, was 0.3 [tesla] in peak magnitude and 0.5 [m] in diameter. [Right] The field was placed at the jet middle and center, was 0.5 [tesla] in peak magnitude and 0.5 [m] in diameter

Obr. 8 [Vlevo] Referenční rychlost lití 4 [m/min]. [Uprostřed] Magnetické pole bylo umístěno v blízkosti vstupu a středu proudu, mělo hodnotu 0,3 [tesla] v píku a průměr 0,5 [m]. [Vpravo] Magnetické pole bylo umístěno uprostřed proudu, mělo š hodnotu 0,5 [tesla] v píku a průměr 0,5 [m]

Tab. 2 presents the coefficients of a quadratic regression model (as defined in Equation 4), which predicts the behavior of the monitored variables as functions of all five input variables. All input variables are normalized within the range [-1, 1]. Examining the linear terms, naturally casting speed (x_u) is the most dominant factor as it strongly increases nearly all monitored variables, particularly total force and jet velocity, while slightly reducing jet deflection. This is reflected in the large, positive values of k_u. The magnetic field's (x_{xc}) position and intensity (x_{B0}) both reduce the meniscus average velocity and jet velocity, with similar magnitudes (k_{xc} = -0.013, k_{B0} = -0.019).

Hutnické listy – *Metallurgical Journal*
Speciální vydání / Special Issue, roč. / vol. LXXIX
ISSN Online: 3029-8350

Field placement near the inlet (higher x_{xc}) also deflects the jet downward. In contrast, positioning the field below the jet (higher x_{zc}) increases both the meniscus average velocity and jet velocity, while deflecting the jet upward. Increasing either the field intensity or coil diameter reduces all output variables and deflects the jet downward, with closly similar impacts. However, these trends based solely on linear terms do not capture the full system behavior. Interaction and nonlinear (quadratic) effects are substantial, particularly for x_{zc}, x_D, and x_{B_0}. For instance, the impact of vertical field placement (x_{zc}) is amplified when combined with changes in field intensity or coil diameter, as seen in the large interaction coefficients k_{zc}: B0 and k_{zc}: D.

$$\begin{aligned} y_r = {} & k_{xc}x_{xc} + k_{zc}x_{zc} + k_D x_D + k_{B0}x_{B_0} + k_u x_u + k_{xc:zc}x_{xc}x_{zc} + k_{xc:D}x_{xc}x_D \\ & + k_{xc:B0}x_{xc}x_{B0} + k_{xc:u}x_{xc}x_u + k_{zc:D}x_{zc}x_D + k_{zc:B0}x_{zc}x_{B0} + k_{D:u}x_D x_{B0} \\ & + k_{B0:u}x_{B0}x_u + k_{xc^2}x_{xc^2} + k_{zc^2}x_{zc^2} + k_{D^2}x_{D^2} + k_{B0^2}x_{B0^2} + k_{u^2}x_{u^2} + k_0 \end{aligned} \quad (4)$$

Tab. 2 Local EMBr regression model coefficients / **Tab. 2** Koeficienty lokálního regresního modelu EMBr

Half-mould	Max. steel Level [m]	Tot. Force (on narrow side) [N]	Meniscus Max. Velocity [m/s]	Meniscus Avg. Velocity [m/s]	Jet def. [m]	Jet Velocity [m/s]	Lower role Velocity [m/s]
k_0	1.662	10461.041	0.482	0.216	0.02	0.652	0.452
k_{xc}	-0.001	-2.122	-0.025	-0.013	-0.014	-0.009	-0.006
k_{zc}	0.002	13.851	0.048	0.017	0.012	0.033	-0.009
k_D	-0.002	-28.141	-0.075	-0.02	0.009	-0.052	-0.027
k_{B0}	-0.002	-36.47	-0.085	-0.019	0.018	-0.073	-0.032
k_u	0.014	189.175	0.322	0.139	-0.011	0.369	0.261
$k_{xc:zc}$	0	3.279	-0.012	0.004	-0.003	0.004	0.005
$k_{xc:D}$	-0.001	-2.207	-0.011	-0.015	-0.015	-0.012	-0.002
$k_{xc:B0}$	-0.002	-6.575	-0.049	-0.019	-0.012	-0.025	-0.006
$k_{xc:u}$	0	5.36	0.017	0.001	0.007	0.019	0.004
$k_{zc:D}$	0.001	15.832	0.037	0.012	0.008	0.031	0.001
$k_{zc:B0}$	0.002	21.375	0.046	0.018	0.018	0.055	-0.014
$k_{zc:u}$	0	1.348	-0.015	-0.002	-0.01	-0.014	-0.006
$k_{D:B0}$	-0.001	-17.544	-0.041	-0.019	0.015	-0.032	-0.027
$k_{D:u}$	-0.001	-17.177	-0.007	-0.001	-0.01	-0.013	-0.001
$k_{B0:u}$	-0.002	-27.79	-0.034	-0.007	-0.015	-0.046	-0.01
k_{x^2}	0	-1.752	0.02	-0.005	-0.005	0.016	0.002
k_{zc^2}	0.001	15.915	0.035	-0.001	-0.022	0.044	0.011
k_{D^2}	0	2.251	0.015	-0.007	-0.004	0.01	-0.001
k_{B0^2}	0	-1.595	0.014	-0.004	0.004	0.005	-0.003
k_{u^2}	0.004	61.513	0.018	0.006	0.005	0.024	0.005

Hutnické listy – *Metallurgical Journal*
Speciální vydání / Special Issue, roč. / vol. LXXIX
ISSN Online: 3029-8350

4. Conclusion

A numerical model was developed to couple electromagnetic effects with molten steel flow within a thin-slab casting mould. The impact of the localized electromagnetic brake (EMBr) is summarized in the **Tab. 3** below.

1. Near Inlet Placement:
   - Results in a slight reduction in molten steel level and overall flow damping, as seen by reductions in force on the narrow face, lower role velocity, meniscus velocity, and jet velocity.
   - The jet is deflected downward, likely due to flow suppression near the inlet.
2. Below Jet Placement:
   - Tends to increase molten steel level, meniscus velocity and force on the narrow side, while decreasing lower role velocity.
   - Meniscus and jet velocities increase, with an upward jet deflection, indicating enhanced upward flow momentum near the meniscus due to deeper magnetic interaction.
3. Larger Diameter (EMBr coils):
   - Causes slight reductions across most parameters, suggesting a more distributed but weaker magnetic braking effect.
   - Jet deflects upward, possibly due to a broader but less intense magnetic influence.
4. Higher Intensity (Magnetic field):
   - Similarly to larger diameter, it shows reductions in flow-related parameters, with upward jet deflection.
   - Indicates stronger suppression of turbulent jet dynamics due to increased magnetic force.

Tab. 3 A summary of local EMBr application effects / **Tab. 3** Souhrn účinků lokální aplikace EMBr

Field parameter	Molten steel level	Force on the narrow side	Lower role velocity	Meniscus average velocity	Jet deflection	Jet velocity
Near inlet placement	Sightly Reduced	Reduced	Reduced	Reduced	Downward	Reduced
Below jet placement	Slightly Increased	Increased	Decreased	Increased	Upward	Increased
Larger diameter	Slightly Reduced	Reduced	Reduced	Reduced	Upward	Reduced
Higher intensity	Slightly Reduced	Reduced	Reduced	Reduced	Upward	Reduced

References

[1] A.R. A. Aziz and S. A. Aziz, 2018. IOP Conf. Ser.: Mater. Sci. Eng. 454 012001
[1] ANSYS, Inc, 2013. ANSYS Fluent Manetohydrodynamics (MHD) Module Manual. Available at: ANSYS FLUENT 12.0 Magnetohydrodynamics Module Manual [Accessed 10 June 2025]
[2] Brian G. Thomas. Introduction to Continuous Casting. Available at: Intro to Continuous Casting - CCC - U of I [Accessed 15 June 2025]
[3] Johan E. Carlson, 2022. Measurement systems Engineering. 2nd ed. Sweden: JEC Engineering and Media Production AB.
[4] Seong-Mook Cho, 2019. "Electromagnetic Forces in Continuous Casting of Steel Slabs". metals.